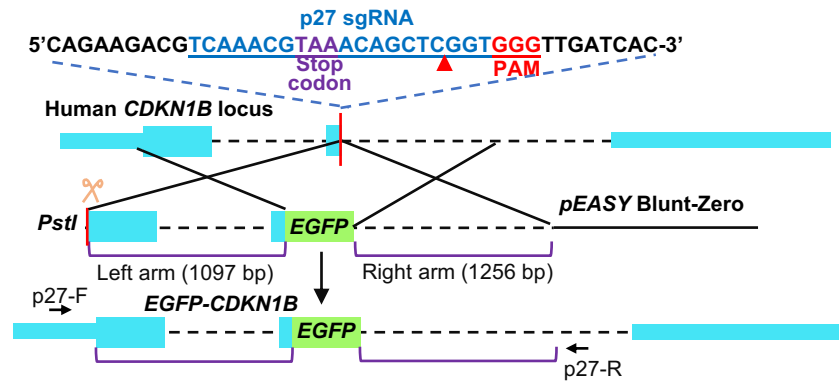
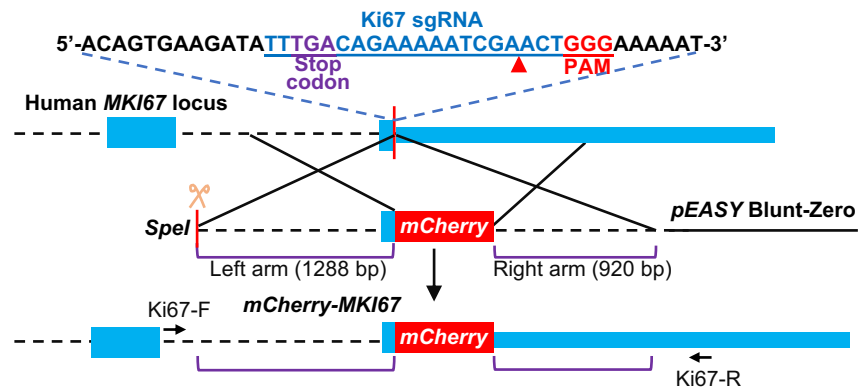


**A**



**B**



**Figure S1. Schematics of the targeting strategy to insert *EGFP* and *mCherry* sequences into the endogenous *CDKN1B* and *MKI67* loci, respectively, via homologous recombination.** The sgRNA sequences (underlined) were designed to span across the stop codons (TAA or TGA) of the endogenous *CDKN1B* or *MKI67*, respectively. Protospacer adjacent motif (PAM) sequences were marked in red. The restriction enzyme *PstI* or *SpeI* were used to linearize the targeting (donor) vectors. The PCR primers (p27-F + p27-R and Ki67-F + Ki67-R) used for genotyping are indicated with horizontal arrows. The left and right homology arms were marked with purple lines. p27-F: Forward primer for EGFP-p27 genotyping; p27-R: Reverse primer for EGFP-p27 genotyping; Ki67-F: Forward primer for mCherry-Ki67 genotyping; Ki67-R: Reverse primer for mCherry-Ki67 genotyping.

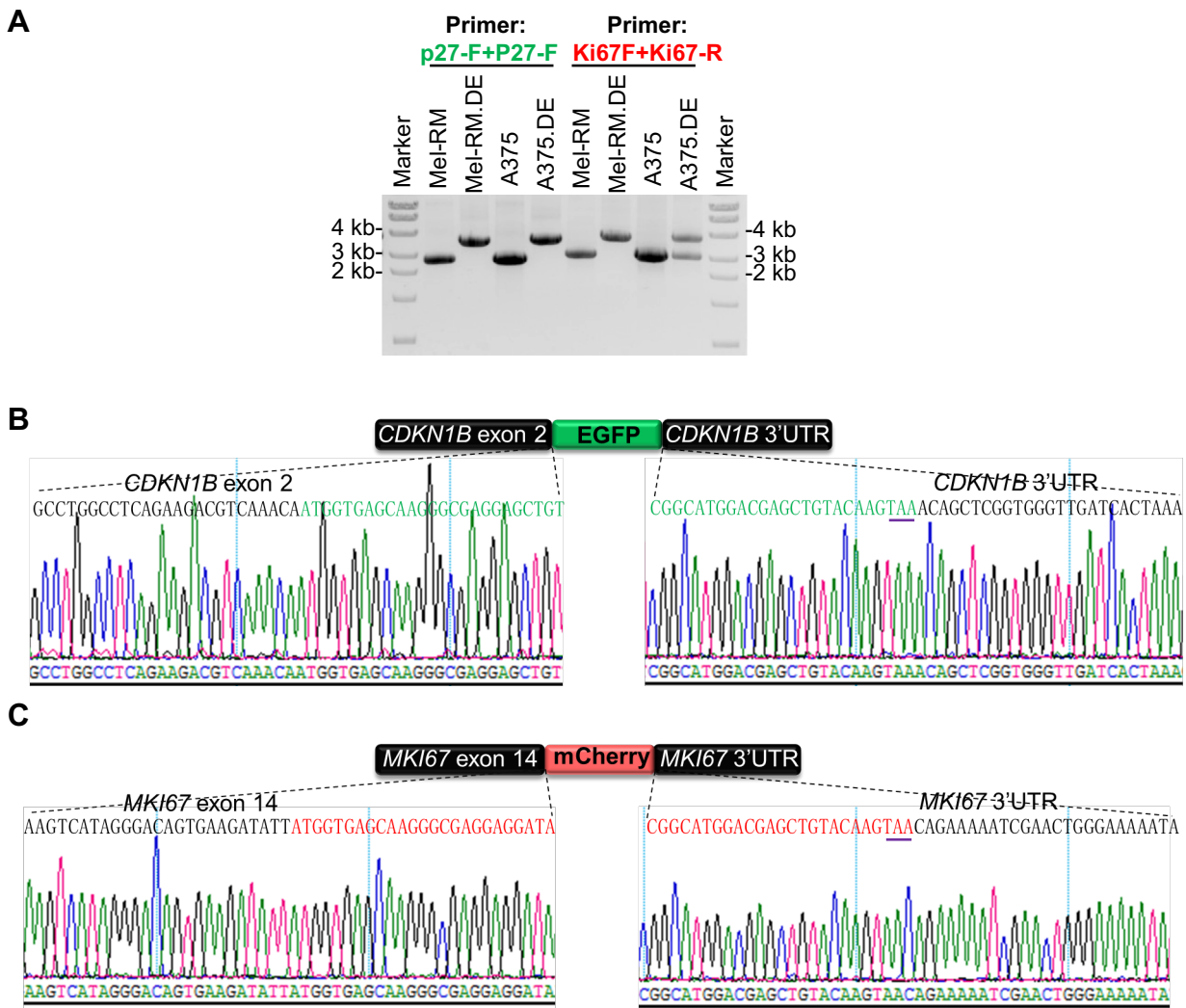


**Figure S2. PCR and Sanger sequencing to confirm the accurate insertion of the *EGFP* and *mCherry* sequences at the C-termini of *CDKN1B* and *MKI67*, respectively.** (A) PCR analysis of the targeted alleles containing the *EGFP* and *mCherry* sequences in dually edited Mel-RM (Mel-RM.DE) and A375 (A375.DE) cells.  $n = 3$ . The primers used were illustrated in Figure S1. (B and C) Sanger sequencing demonstrated the precise integration of *EGFP* (B) and *mCherry* (C) at the C-termini of *CDKN1B* (B) and *MKI67* (C), respectively. The stop codons are underlined.

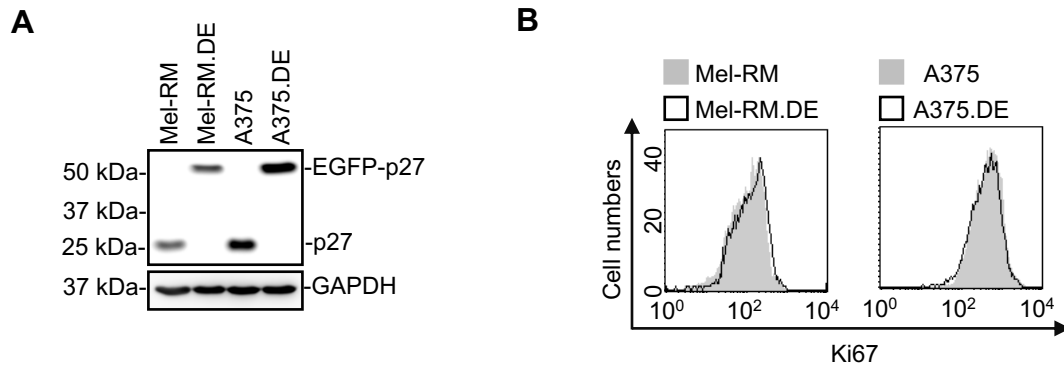


**Figure S3. The levels of p27 and Ki67 expression remain unaltered in dually edited cells.** (A) Whole cell lysates from parental Mel-RM and A375 and dually edited Mel-RM (Mel-RM.DE) and A375 (A375.DE) cells were analysed using Western blotting.  $n = 3$ . (B) Representative flowcytometric histograms showing the dually edited cells and corresponding parental cells expressed similar levels of Ki67 identified using an APC conjugated anti-Ki-67 antibody.  $n = 3$ .

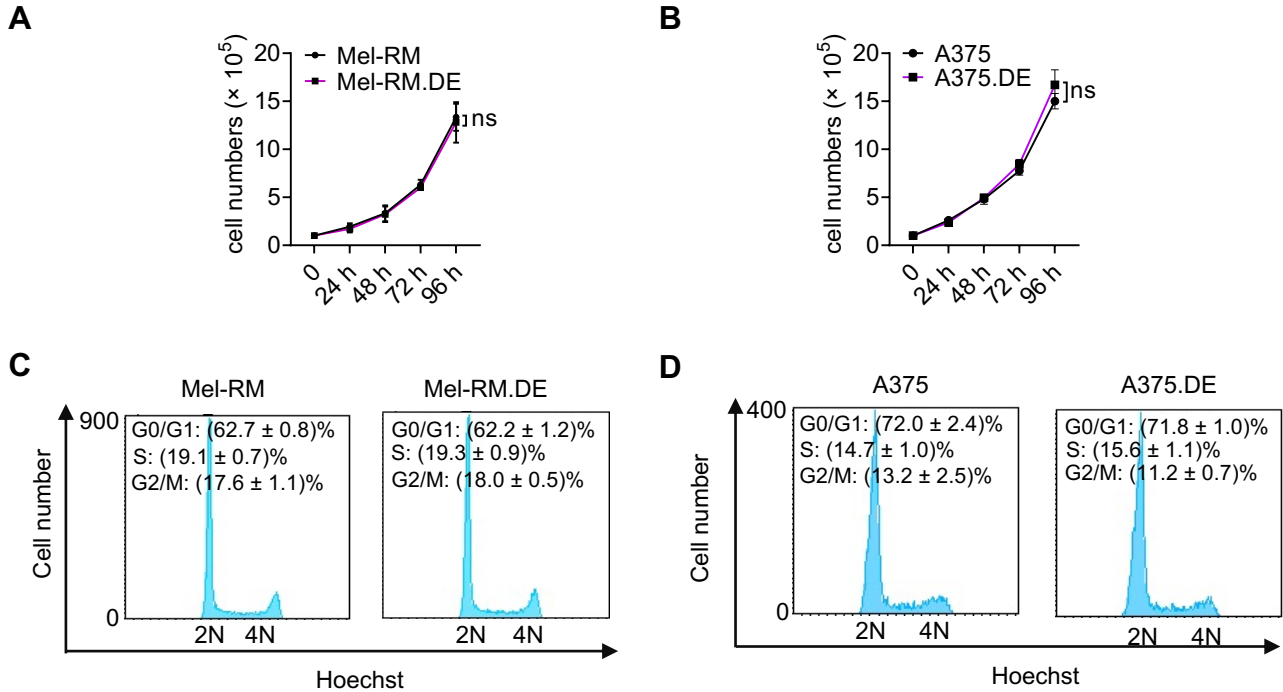


**Figure S4. The proliferation rate and cell cycle distribution remain unaltered in dually edited cells.** (A and B) Viable parental Mel-RM and A375 and dually edited Mel-RM (Mel-RM.DE) and A375 (A375.DE) cells were counted using an automated cell counter 24, 48, 72, and 96 h after seeding. Values are mean ± SDs,  $n = 3$  ( $P > 0.05$ , two-tailed Student's  $t$ -test). (C and D) Mel-RM, Mel-RM.DE, A375 and A375.DE cells were subjected to Propidium iodide (PI) analysis of cell cycle distribution using flow cytometer. Values are mean ± SDs;  $n = 3$ .

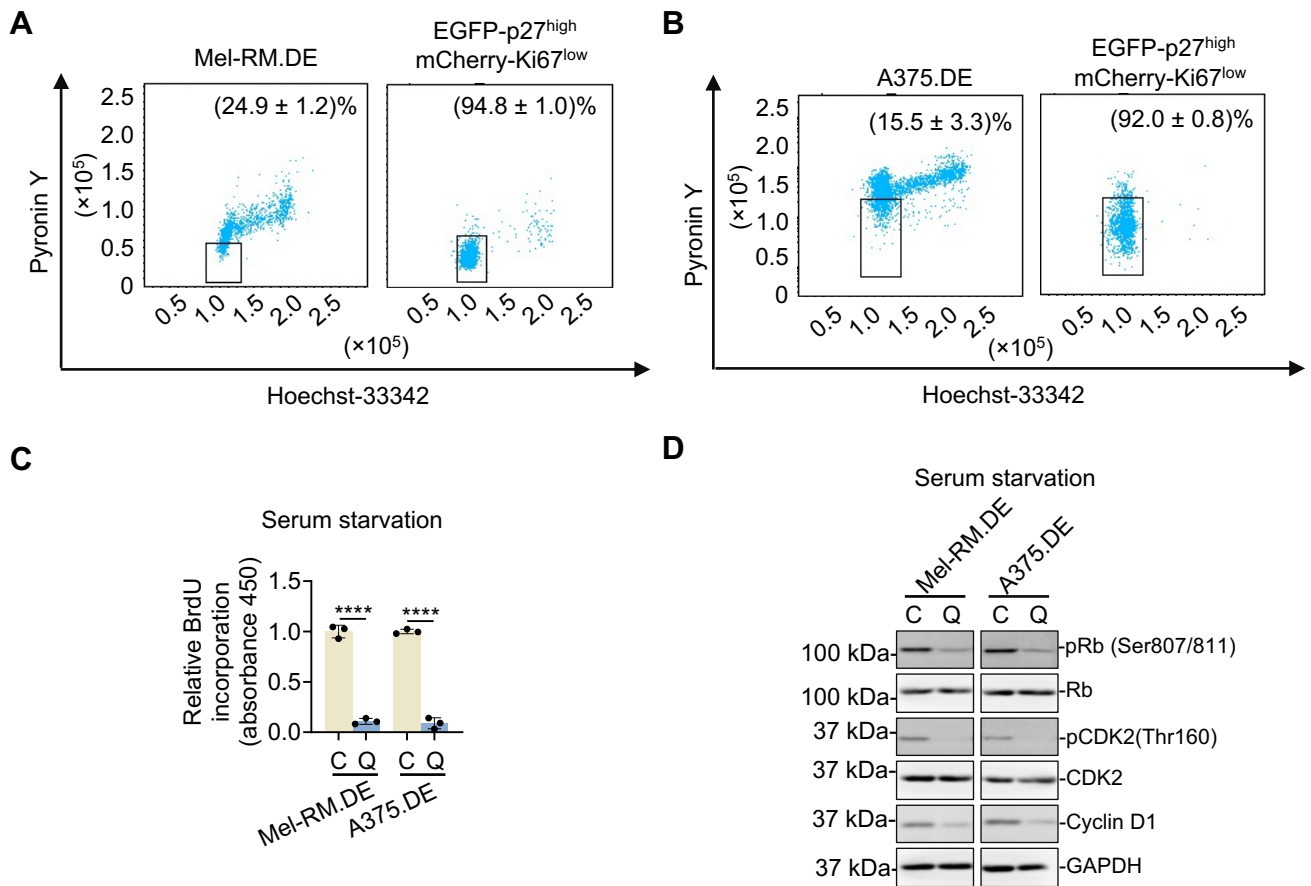


**Figure S5. EGFP-p27<sup>high</sup>mCherry-Ki67<sup>low</sup> cells display quiescent characteristics.** (A and B) Representative flowcytometry dot plots of EGFP-p27<sup>high</sup>mCherry-Ki67<sup>low</sup> cells isolated from dually edited Mel-RM (Mel-RM.DE; A) and A375 (A375.DE ;B) cells with DNA and RNA labelled using Hoechst-33342 and Pyronin Y staining, respectively. Values are mean  $\pm$  SDs;  $n = 3$ . (C) The DNA synthesis activity was not detected in EGFP-p27<sup>high</sup>mCherry-Ki67<sup>low</sup> [quiescent cells (Q)] cells, but was readily detectable in the other cells [cycling cells (C)] isolated from Mel-RM.DE and A375.DE cells upon serum starvation as shown in BrdU incorporation assays. Values are mean  $\pm$  SDs;  $n = 3$  (\*\*\*\* $P < 0.0001$ , two-tailed Student's  $t$ -test). (D) Whole cell lysates from EGFP-p27<sup>high</sup>mCherry-Ki67<sup>low</sup> quiescent (Q) and cycling cells isolated from Mel-RM.DE and A375.DE cells undergoing serum starvation were subjected to Western blotting.  $n = 3$ .

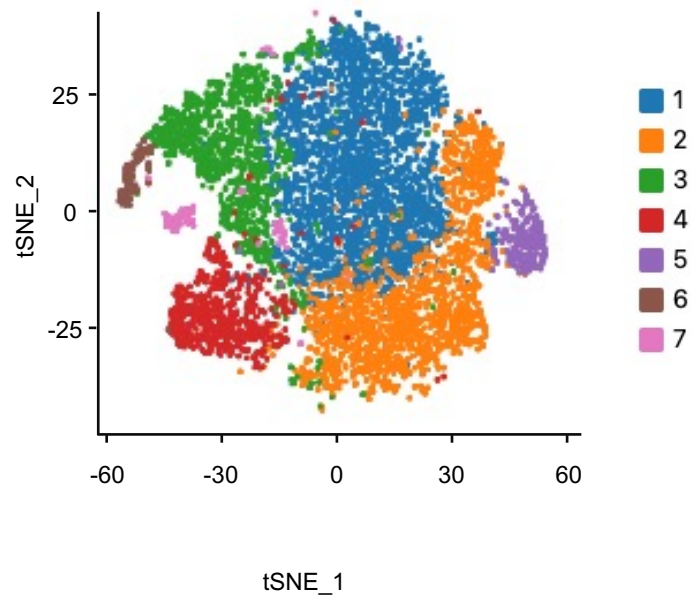


**Figure S6.** t-Distributed stochastic neighbor embedding (t-SNE) visualization of transcriptomes of 7554 single EGFP-p27<sup>high</sup>mCherry-Ki67<sup>low</sup> quiescent cells isolated from dually edited Mel-RM cells upon serum starvation. Cells are colored by their associated clusters (1-7).

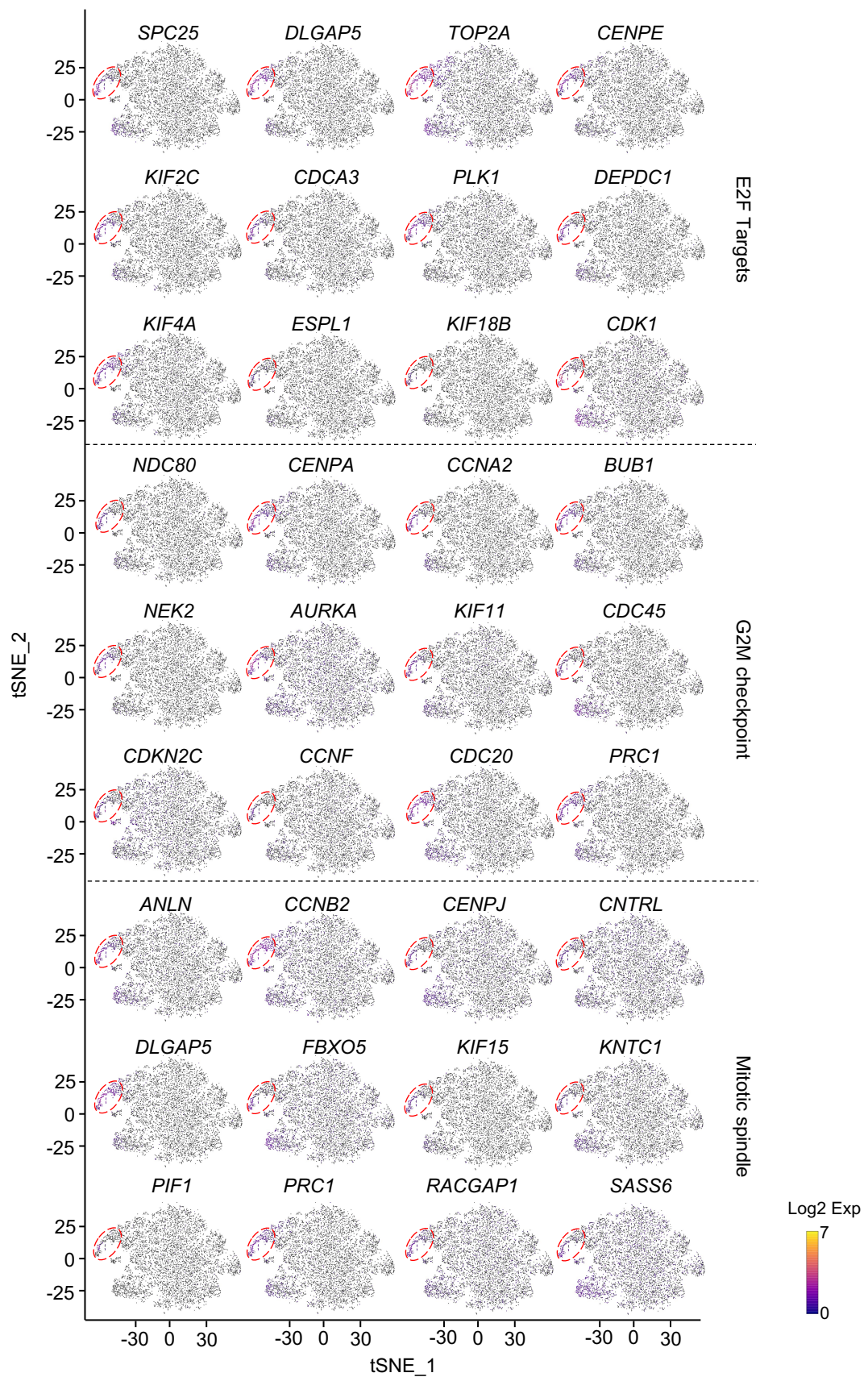


**Figure S7. EGFP-p27<sup>high</sup>mCherry-Ki67<sup>low</sup> cells express no or low levels of representative E2F, G2M checkpoint and mitotic spindle assembly pathway genes.** t-SNE plots of single cell RNA-sequencing data showing that representative genes of the E2F, G2M checkpoint and mitotic spindle assembly pathways were not expressed or detected at low levels in the majority of EGFP-p27<sup>high</sup>mCherry-Ki67<sup>low</sup> cells isolated from dually edited Mel-RM cells undergoing serum starvation. A small population of cells that expressed relatively high levels of these genes are marked by ellipses.

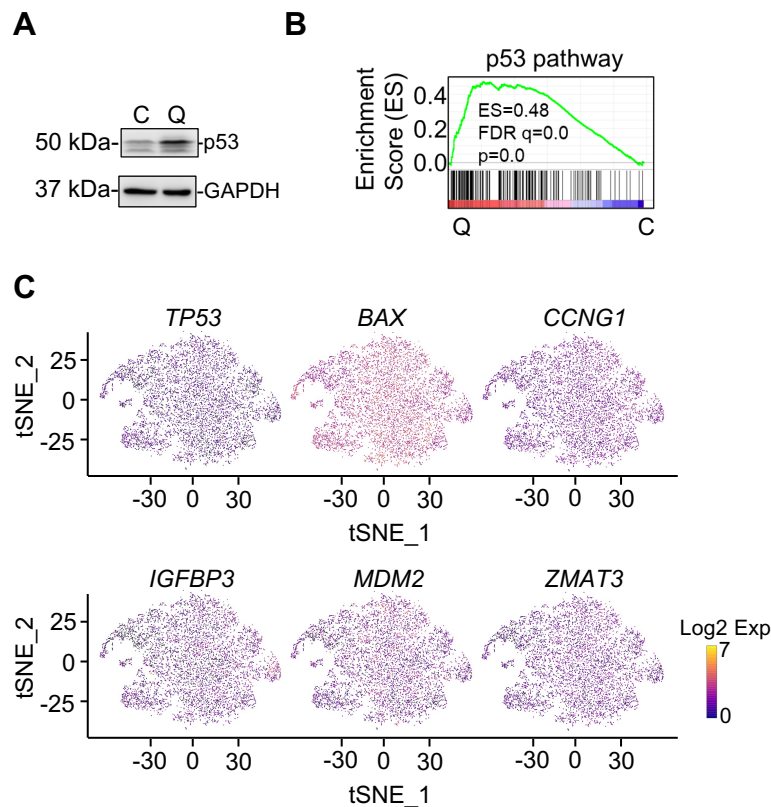


**Figure S8. The p53 pathway is enriched in quiescent cells.** (A) Whole cell lysates from EGFP-p27<sup>high</sup>mCherry-Ki67<sup>low</sup> quiescent (Q) and cycling (C) cells isolated from dually edited Mel-RM cells undergoing serum starvation were analysed using Western blotting.  $n = 3$ . (B) A GSEA plot of bulk cell RNA-sequencing (bcRNA-seq) data showing that the p53 pathway was enriched in EGFP-p27<sup>high</sup>mCherry-Ki67<sup>low</sup> quiescent (Q) compared with cycling (C) cells isolated from dually edited Mel-RM cells undergoing serum starvation. FDR, false-discovery rate; ES, enrichment score.  $n = 2$  biological repeats. (C) t-SNE plots of single cell RNA-sequencing (scRNA-seq) data showing that *TP53* and representative p53 target genes were expressed in EGFP-p27<sup>high</sup>mCherry-Ki67<sup>low</sup> quiescent cells isolated from dually edited Mel-RM cells undergoing serum starvation.

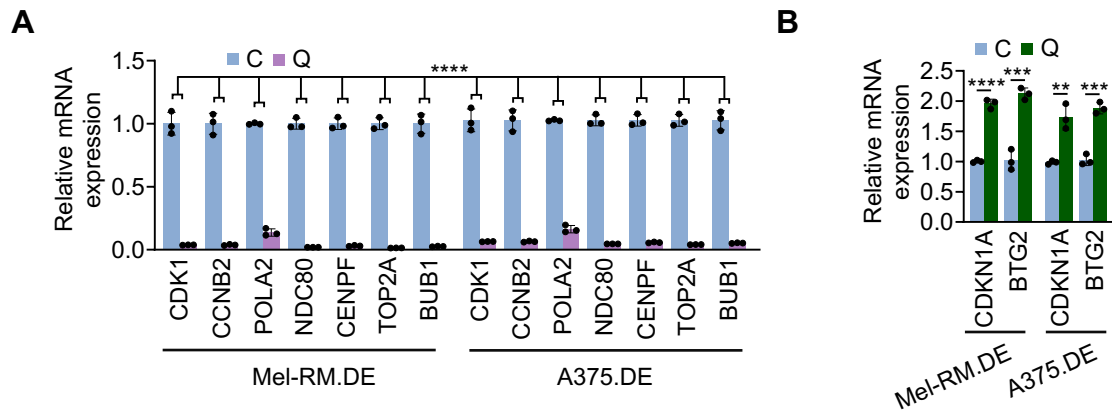


**Figure S9. Validation of the changes in representative E2F, G2M progression, mitotic spindle assembly and p53 pathway genes in quiescent compared with cycling cells.** Total RNA from EGFP-p27<sup>high</sup>mCherry-Ki67<sup>low</sup> quiescent (Q) and cycling (C) cells isolated from dually edited Mel-RM (Mel-RM.DE) and A375 (A375.DE) cells undergoing serum starvation were subjected to qPCR analysis of the indicated representative E2F, G2M progression, mitotic spindle assembly pathway genes (A) and p53 pathway genes (B). Values are mean  $\pm$  SDs;  $n = 3$  (\*\* $P < 0.01$ ; \*\*\* $P < 0.001$ ; \*\*\*\* $P < 0.0001$ , two-tailed Student's  $t$ -test).

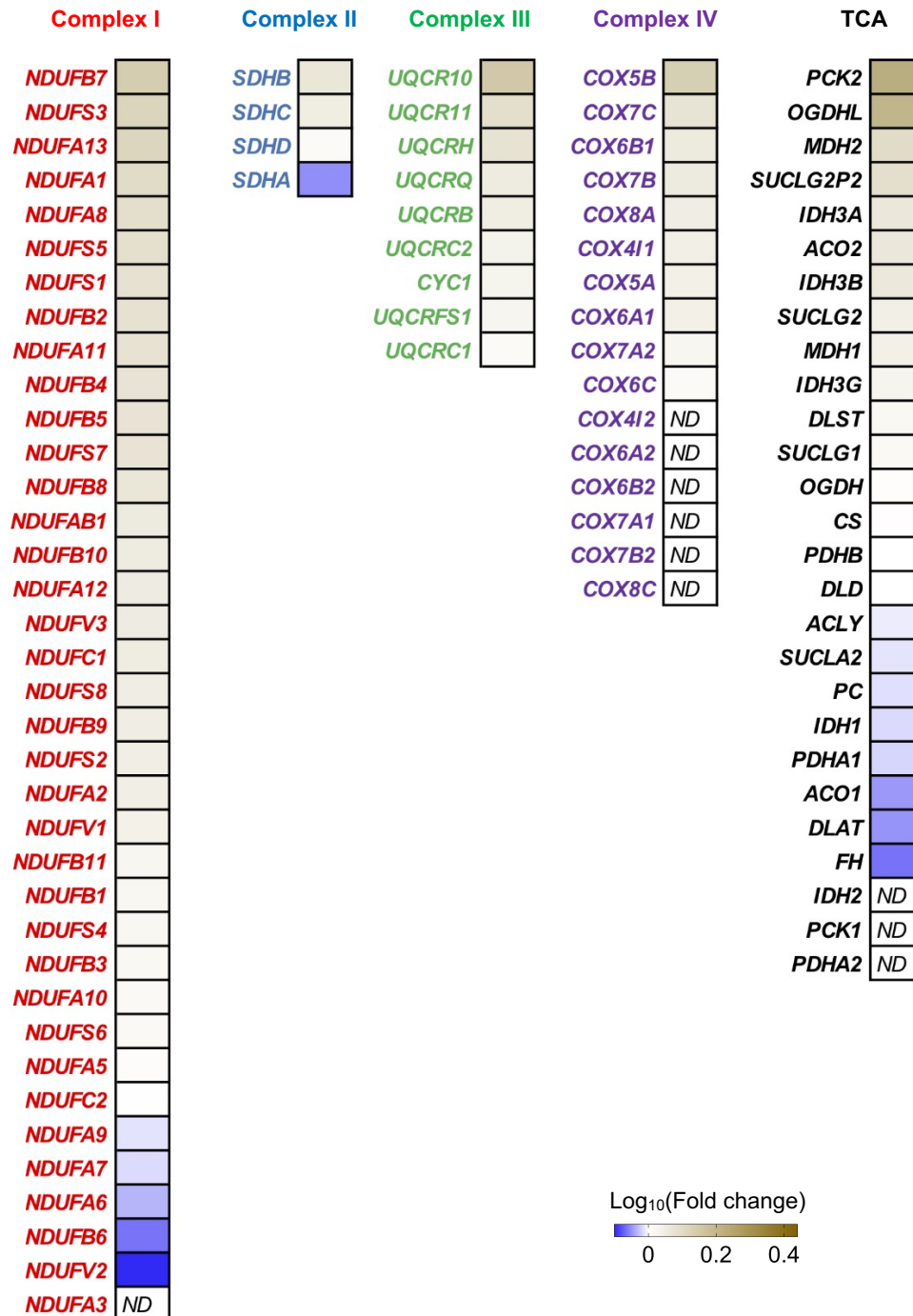


**Figure S10. Upregulation of OXPHOS and TCA genes in quiescent cells.** Log<sub>10</sub>-transformed fold gene expression changes derived from bulk cell RNA-sequencing of EGFP-p27<sup>high</sup>mCherry-Ki67<sup>low</sup> quiescent and cycling cells isolated from dually edited Mel-RM cells undergoing serum starvation were subjected to hierarchical clustering and displayed in the thumbnail-dendrogram format. *n* = 2 biological repeats. *ND*: not detectable by RNA-seq.

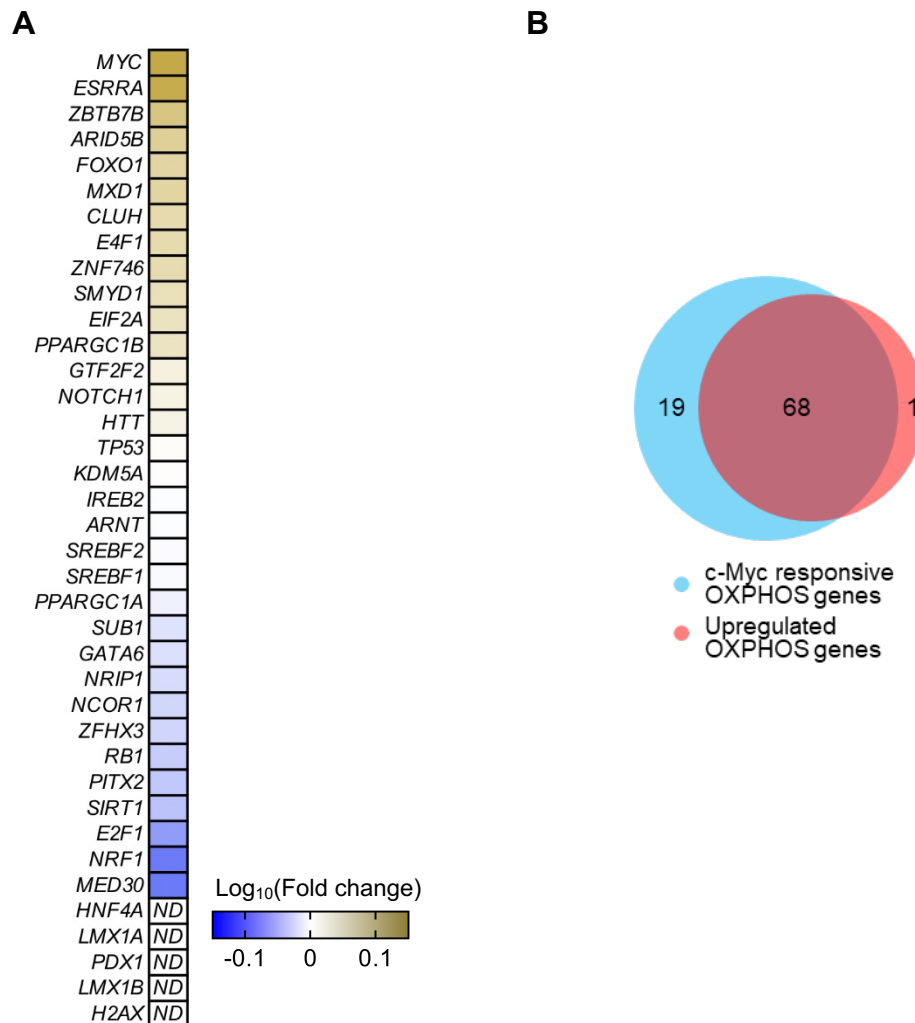


**Figure S11. *MYC* and c-Myc-responsive OXPPOS genes are expressed at higher levels in quiescent compared with cycling cells. (A)** Log<sub>10</sub>-transformed fold gene expression changes derived from bulk cell RNA-sequencing of EGFP-p27<sup>high</sup>mCherry-Ki67<sup>low</sup> quiescent and cycling cells isolated from dually edited Mel-RM cells undergoing serum starvation were subjected to hierarchical clustering and displayed in the thumbnail-dendrogram format. *MYC* was the most prominently upregulated gene among those encoding transcription factors that regulate OXPPOS gene expression in EGFP-p27<sup>high</sup>mCherry-Ki67<sup>low</sup> quiescent compared to cycling cells. *n* = 2 biological repeats. **(B)** Venn diagram illustrating that almost all OXPPOS genes that were upregulated in EGFP-p27<sup>high</sup>mCherry-Ki67<sup>low</sup> quiescent compared to cycling cells isolated from dually edited Mel-RM cells undergoing serum starvation were those that c-Myc-responsive genes. c-Myc responsive genes were defined according to the Encyclopedia of DNA Elements (ENCODE) transcription factor binding sites (TFBS) chromatin immunoprecipitation (ChIP)-seq data.

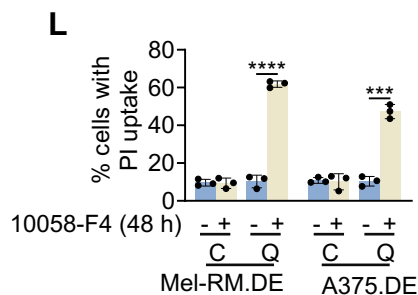
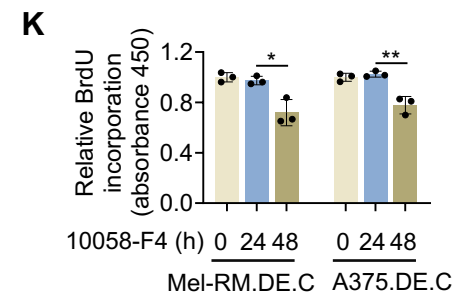
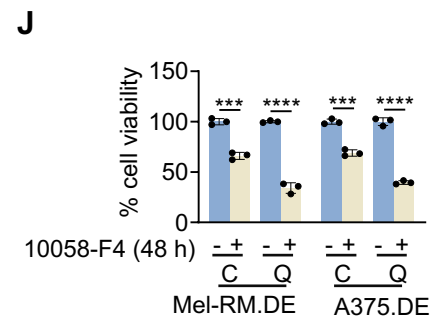
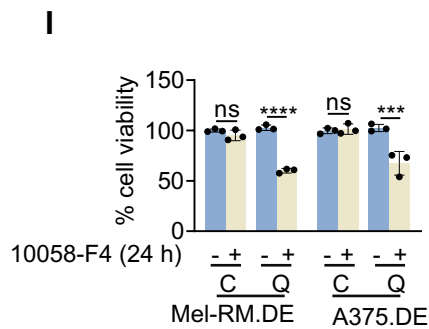
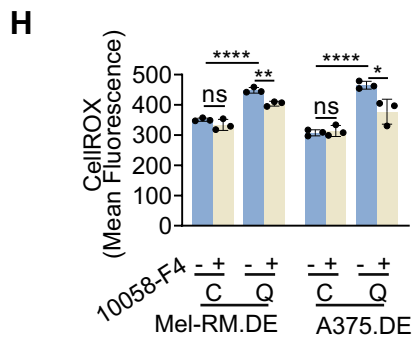
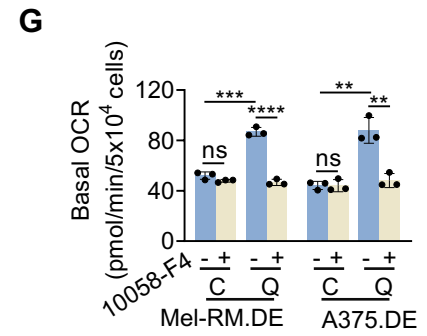
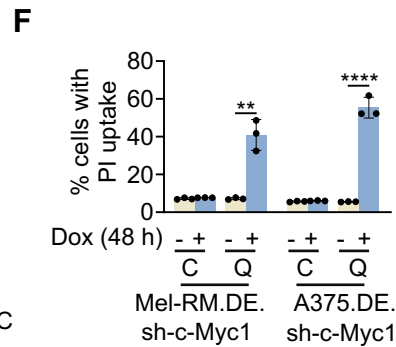
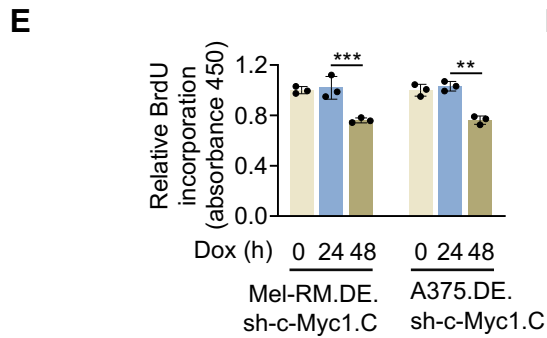
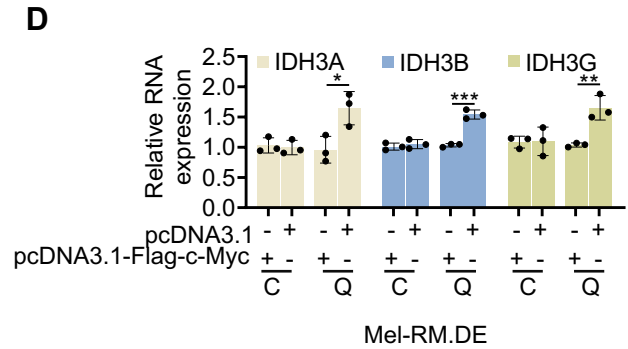
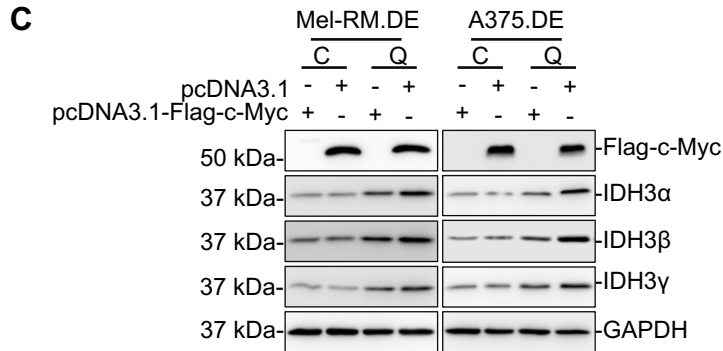
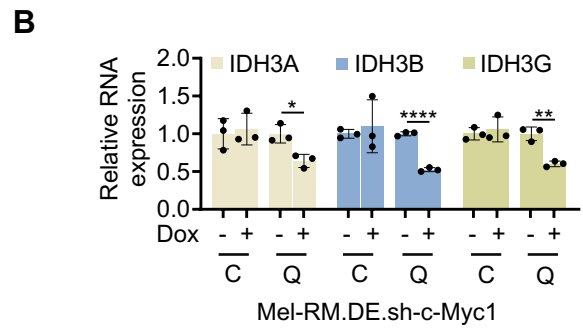
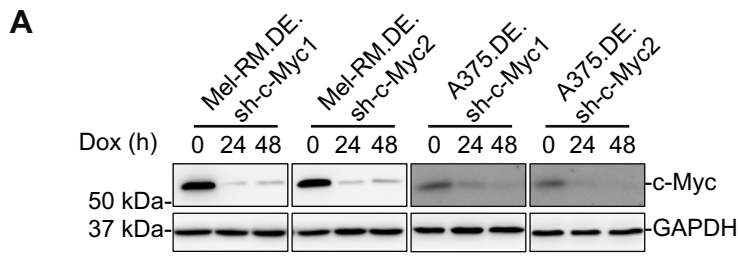


**Figure S12. c-Myc drives OXPHOS and promotes cell survival in quiescent cells.** (A) Whole cell lysates from dually edited Mel-RM (Mel-RM.DE) and A375 (A375.DE) cells carrying an inducible c-Myc shRNA system with or without treatment with Doxycycline (Dox; 100ng/ml) for the indicated periods were subjected to Western blotting.  $n = 3$ . (B) Total RNA from EGFP-p27<sup>high</sup>mCherry-Ki67<sup>low</sup> quiescent (Q) and cycling (C) cells isolated from Mel-RM.DE and A375.DE cells carrying an inducible c-Myc shRNA system with or without treatment with Doxycycline (Dox) for 24 h undergoing serum starvation were subjected to qPCR analysis. Values are mean  $\pm$  SDs;  $n = 3$  ( $*P < 0.05$ ;  $**P < 0.01$   $****P < 0.0001$ , two-tailed Student's  $t$ -test). (C) Whole cell lysates from EGFP-p27<sup>high</sup>mCherry-Ki67<sup>low</sup> quiescent (Q) and cycling (C) cells isolated from Mel-RM.DE and A375.DE cells transfected with the indicated plasmids undergoing serum starvation were analyzed using Western blotting.  $n = 3$ . (D) Total RNA from EGFP-p27<sup>high</sup>mCherry-Ki67<sup>low</sup> quiescent (Q) cells isolated from Mel-RM.DE cells transfected with the indicated plasmids undergoing serum starvation were subjected to qPCR analysis. Values are mean  $\pm$  SDs;  $n = 3$  ( $*P < 0.05$ ;  $**P < 0.01$ ,  $***P < 0.001$ , two-tailed Student's  $t$ -test). (E) EGFP-p27<sup>low</sup>mCherry-Ki67<sup>high</sup> cycling cells isolated from Mel-RM.DE (Mel-RM.DE.C) and A375.DE (A375.DE.C) cells carrying an inducible c-Myc shRNA system undergoing serum starvation were treated with Dox for the indicated periods were subjected to measurement of DNA synthesis using BrdU incorporation assays. The relative BrdU incorporation in cells of each cell line without Dox treatment was arbitrarily designated as 1, respectively. Values are mean  $\pm$  SDs;  $n = 3$  ( $**P < 0.01$ ;  $***P < 0.001$ , two-tailed Student's  $t$ -test). (F) EGFP-p27<sup>high</sup>mCherry-Ki67<sup>low</sup> quiescent (Q) and cycling (C) cells isolated from Mel-RM.DE and A375.DE cells carrying an inducible c-Myc shRNA system undergoing serum starvation were treated with Dox for 48 h before cell death was measured using the PI uptake assay. Values are mean  $\pm$  SDs;  $n = 3$  ( $**P < 0.01$ ;  $****P < 0.0001$ , two-tailed Student's  $t$ -test). (G) The basal oxygen consumption rate (OCR) measured using Seahorse XF analysis of EGFP-p27<sup>high</sup>mCherry-Ki67<sup>low</sup> quiescent (Q) and cycling (C) cells isolated from Mel-RM.DE and A375.DE cells undergoing serum starvation for 96 h with or without treatment with 10058-F4 for 24 h. Values are mean  $\pm$  SDs;  $n = 3$  ( $**P < 0.01$ ;  $***P < 0.001$ ;  $****P < 0.0001$ , two-tailed Student's  $t$ -test). (H) EGFP-p27<sup>high</sup>mCherry-Ki67<sup>low</sup> quiescent (Q) and cycling (C) cells isolated from Mel-RM.DE and A375.DE cells undergoing serum starvation for 96 h with or without treatment with 10058-F4 for 24 h were subjected to CellROX analysis of oxidative stress levels. Values are mean  $\pm$  SDs;  $n = 3$  ( $*P < 0.05$ ;  $**P < 0.01$ ;  $****P < 0.0001$ , two-tailed Student's  $t$ -test). (I) EGFP-p27<sup>high</sup>mCherry-Ki67<sup>low</sup> quiescent (Q) and cycling (C) cells isolated from Mel-RM.DE and A375.DE cells undergoing serum starvation for 96 h with or without treatment with 10058-F4 for 24 h were subjected to CCK8 assays. Values are mean  $\pm$  SDs;  $n = 3$  ( $****P < 0.001$   $****P < 0.0001$ , two-tailed Student's  $t$ -test). (J) EGFP-p27<sup>high</sup>mCherry-Ki67<sup>low</sup> quiescent (Q) and cycling (C) cells isolated from Mel-RM.DE and A375.DE cells undergoing serum starvation in the presence or absence of 10058-F4 for 48 h were subjected to measurement of cell viability using CCK8 assays). Values are mean  $\pm$  SDs;  $n = 3$  ( $****P < 0.001$   $****P < 0.0001$ , two-tailed Student's  $t$ -test). (K) EGFP-p27<sup>low</sup>mCherry-Ki67<sup>high</sup> cycling cells isolated from Mel-RM.DE (Mel-RM.DE.C) and A375.DE (A375.DE.C) cells undergoing serum starvation were treated with 10058-F4 for the indicated periods were subjected to BrdU incorporation assays as described for (E). The relative BrdU incorporation in cells of each cell line without treatment was arbitrarily designated as 1, respectively. Values are mean  $\pm$  SDs;  $n = 3$  ( $*P < 0.05$   $**P < 0.01$ , two-tailed Student's  $t$ -test). (L) EGFP-p27<sup>high</sup>mCherry-Ki67<sup>low</sup> quiescent (Q) and cycling (C) cells isolated from Mel-RM.DE and A375.DE cells undergoing serum starvation in the presence or absence of 10058-F4 for 48 h was measured using the PI uptake assay. Values are mean  $\pm$  SDs;  $n = 3$  ( $**P < 0.01$ ;  $****P < 0.0001$ , two-tailed Student's  $t$ -test).

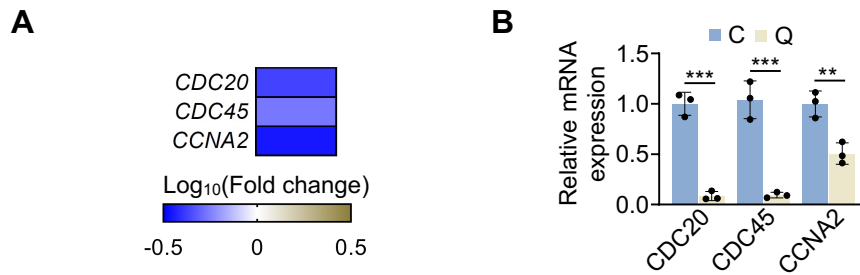


**Figure S13. c-Myc-responsive cell proliferation genes are expressed at low levels in quiescent cells.** (A) Log<sub>10</sub>-transformed fold gene expression changes derived from bulk cell RNA-sequencing of EGFP-p27<sup>high</sup>mCherry-Ki67<sup>low</sup> quiescent and cycling cells isolated from dually edited Mel-RM cells undergoing serum starvation were subjected to hierarchical clustering and displayed in the thumbnail-dendrogram format.  $n = 2$  biological repeats. (B) Total RNA from EGFP-p27<sup>high</sup>mCherry-Ki67<sup>low</sup> quiescent (Q) and cycling (C) cells isolated from dually edited Mel-RM cells undergoing serum starvation were subjected to qPCR analysis. Values are mean  $\pm$  SDs;  $n = 3$  (\*\* $P < 0.01$ ; \*\*\* $P < 0.001$ , two-tailed Student's  $t$ -test).

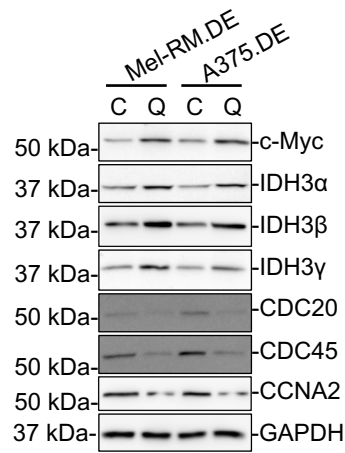


**Figure S14. EGFP-p27<sup>high</sup>mCherry-Ki67<sup>low</sup> cells grown in 3-dimensional (3-D) cultures display higher levels of IDH3 and lower levels cell cycle progression genes.** Whole cell lysates from EGFP-p27<sup>high</sup>mCherry-Ki67<sup>low</sup> quiescent (Q) and cycling (C) cells isolated from Mel-RM.DE and A375.DE cells grown in 3-D cultures subjected to serum starvation were subjected to Western blotting. *n* = 3.

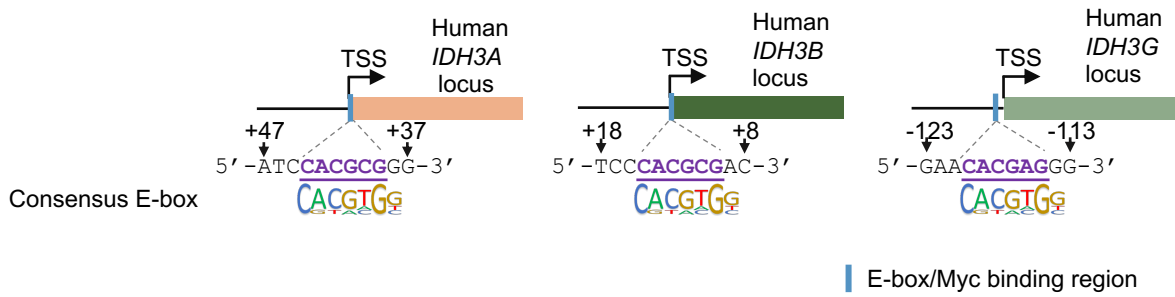


**Figure S15.** A schematic illustration of consensus E-box/c-Myc binding regions in the promoters of *IDH3A*, *IDH3B* and *IDH3G*.

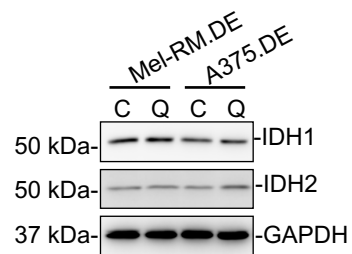


**Figure S16. IDH1 and IDH2 expression remain unaltered in quiescent cells.** Whole cell lysates from EGFP-p27<sup>high</sup>mCherry-Ki67<sup>low</sup> quiescent (Q) and cycling (C) cells isolated from dually edited Mel-RM (Mel-RM.DE) and A375 (A375.DE) cells undergoing serum starvation were subjected to Western blotting.  $n = 3$ .

**Table S1. Oligonucleotides used for sgRNA plasmid construction and genotyping**

Oligo	Sequence (5'-3')
p27 sgRNA-top	CACCGTCAAACGTAAACAGCTCG
p27 sgRNA-bottom	AAACACCGAGCTGTTTACGTTTG
Ki67 sgRNA-top	CACCGTTTGACAGAAAAATCGAA
Ki67 sgRNA-bottom	AAACAGTTCGATTTTTCTGTCAA
p27-F	TTTTTTTGAGAGTGCGAGAGAGG
p27-R	GGTCAAAGGCAAGTGGGAAATA
Ki67-F	GTGAGAGTTCCTGGTCAGTGGGG
Ki67-R	TGGATGACGCTGTGAGAACCCTA

**Table S2. List of Reagents**

<b>Reagent</b>	<b>Catalogue No.</b>	<b>Company</b>
2,4-Dinitrophenol	34334	Sigma-Aldrich
10058-F4	F3680	Sigma-Aldrich
IACS-010759	25867	Cayman
Doxycycline hydrochloride	D3447	Sigma-Aldrich
Puromycin dihydrochloride	P9620	Sigma-Aldrich
bisBenzimide H 33258	B2883-100mg	Sigma-Aldrich
Pyronin Y	P9172-1G	Sigma-Aldrich
Propidium iodide	P4170-1G	Sigma-Aldrich
pEASY® -Blunt Zero Cloning Kit	CB501-01	TransGen Biotech
BrdU Cell Proliferation Assay Kit	#6813	Cell Signaling

**Table S3. List of antibodies**

<b>Antibody</b>	<b>Catalogue No.</b>	<b>Company</b>
Phospho-Rb (Ser807/811) antibody	#9308	Cell Signalling Technology (Beverly, MA)
Recombinant Anti-Rb antibody [EPR17512]	ab181616	Abcam (Cambridge, United Kingdom)
HIF-1 $\alpha$ Antibody (28b)	sc-13515	Santa Cruz Biotechnology (Santa Cruz, CA)
Phospho-CDK2 (Thr160) Antibody	#2561	Cell Signalling Technology (Beverly, MA)
Cdk2 (D-12)	sc-6248	Santa Cruz Biotechnology (Santa Cruz, CA)
cyclin D1 Antibody (H-295)	sc-753	Santa Cruz Biotechnology (Santa Cruz, CA)
p27 Kip1 (D69C12) XP <sup>®</sup> Rabbit mAb	#3686	Cell Signalling Technology (Beverly, MA)
GAPDH antibody (6C5)	sc-32233	Santa Cruz Biotechnology (Santa Cruz, CA)
Anti-IDH3A antibody	ab58641	Abcam (Cambridge, United Kingdom)
Anti-IDH3B antibody	ab247089	Abcam (Cambridge, United Kingdom)
Anti-IDH3G antibody	ab224210	Abcam (Cambridge, United Kingdom)
Recombinant Anti-SDHC antibody [EPR11035(B)]	ab155999	Cell Signalling Technology (Beverly, MA)
Anti-NDUFV1	ab203208	Abcam (Cambridge, United Kingdom)
Recombinant Anti-IDH1 antibody [EPR12296]	ab172964	Abcam (Cambridge, United Kingdom)
Recombinant Anti-IDH2 antibody [EPR7577]	ab131263	Abcam (Cambridge, United Kingdom)
c-Myc Antibody	#9402	Cell Signalling Technology (Beverly, MA)
APC anti-mouse Ki-67 antibody	652406	BioLegend (San Diego, CA)

**Table S4. Oligonucleotides used for qPCR**

Oligo	Sequence (5'-3')
CDK1 qPCR-F	GGTCAAGTGGTAGCCATGAAA
CDK1 qPCR-R	ATGTACTGACCAGGAGGGATAG
CCNB2 qPCR-F	GCAGTCCATAAACCCACATTTC
CCNB2 qPCR-R	GCAGAGCAGTAATCCCAACTA
POLA2 qPCR-F	ATTATCGAAAGCCAGGCATAGT
POLA2 qPCR-R	GAGAAACTTGACGGTGAGAGTA
NDC80 qPCR-F	TCTCTACAAGCTCCCTCTGTTA
NDC80 qPCR-R	CAAACCTAAGGCTGCCACAATG
CENPF qPCR-F	GAGCTTGAAGGACAGCTTGA
CENPF qPCR-R	TCACTTGTGACTCCTTGACTTG
TOP2A qPCR-F	CTGCGGACAACAAACAAAGG
TOP2A qPCR-R	TTCGACCACCTGTCACCTTC
BUB1 qPCR-F	TTGCTCCTCCTGTTCCCTTG
BUB1 qPCR-R	CTGAACCATTCCCAGTGATGT
IDH3A qPCR-F	GCTGCCAAAGCACCTATT
IDH3A qPCR-R	TCAAGCCATCTTGTTCCTTATC
IDH3B qPCR-F	TTGGAAAGATTCATACCCCGAT
IDH3B qPCR-R	TGTTGTGCCGAGTCATATACCC
IDH3G qPCR-F	GTACCAGTGGACTTTGAAGAG
IDH3G qPCR-R	CGGACAATGAGGATGTCTATG
NDUFB7 qPCR-F	GATGCCAACCTTCCC GCCAGA
NDUFB7 qPCR-R	AGCTGTCACGCTTGCACTTGA
SDHB qPCR-F	TGATAAAGGATCTTGTTCCCGAT
SDHB qPCR -R	TTTCTCACGCTCTTCTATGGAC
UQCR10 qPCR-F	ATCTACGACCACATCAACGAGG
UQCR10 qPCR-R	CGTTTCTTGCCAACAGCGAAT
COX5B qPCR-F	CAATGGCTTCAAGGTTACTTCGC
COX5B qPCR-R	CTTTGCAGCCAGCATGATCTCC
c-Myc qPCR-F	TCCGTCCCTCGGATTCTCTGCTCT
c-Myc qPCR-R	GCCTCCAGCAGAAGGTGATCCA
CDC20 qPCR-F	ATCTGGAATGTGTGCTCTGG
CDC20 qPCR-R	CCTGAGATGAGCTCCTTGTAATG
CDC45 qPCR-F	GTCTTTGCCACCATGTCTTTG
CDC45 qPCR-R	GTACAGCTTGTCCAGGTTACTC
CCNA2 qPCR-F	TCACCAGACCTACCTCAA
CCNA2 qPCR-R	GAGGAGAGAAACACCATGATAC

**Table S5. Oligonucleotides used for inducible shRNA plasmid construction**

Oligo	Sequence (5'-3')
sh-IDH3 $\alpha$ 1 top	CTAGCGGTGGTGTTCAGACAGTAATTCAAGAGATTACTGTCTG AACACCACCTTTTTG
sh-IDH3 $\alpha$ 1 bottom	AATTCAAAAAGGTGGTGTTCAGACAGTAATCTCTTGAATTACTG TCTGAACACCACCG
sh-IDH3 $\alpha$ 2 top	CTAGCGCTAAAGAGTCCATGGATATACTAGTTATCCATGGACTC TTTAGCTTTTTG
sh-IDH3 $\alpha$ 2 bottom	AATTCAAAAAGCTAAAGAGTCCATGGATAACTAGTATATCCAT GGACTCTTTAGCG
sh-c-Myc 1 top	CTAGCCCTGAGACAGATCAGCAACAACACTACTAGTGTTGTTGCT GATCTGTCTCAGGTTTTTG
sh-c-Myc 1 bottom	AATTCAAAAACCTGAGACAGATCAGCAACAACACTAGTAGTTG TTGCTGATCTGTCTCAGGG
sh-c-Myc 2 top	CTAGCGGACTATCCTGCTGCCAAGTACTAGTCTTGGCAGCAGG ATAGTCCTTTTTG
sh-c-Myc 2 bottom	AATTCAAAAAGGACTATCCTGCTGCCAAGACTAGTACTTGGCA GCAGGATAGTCCG

**Table S6. Oligonucleotides used for ChIP**

Oligo	Sequence (5'-3')
NDUFB7-ChIP-F	CCTAAATGACCCGGAAGCTG
NDUFB7-ChIP-R	CGAGGGTCACCTAGCTCCTAC
COX5B-ChIP-F	CTCCTGTCTCTGCAGCTTGTTCC
COX5B-ChIP-R	CCGCGAAGTAACCTTGAAGCC
UQCR10-ChIP-F	TCCCATAAAGTGTTGCACGTC
UQCR10-ChIP-R	CGCCATGTTTCTTCACAGTCCA
CCNA2-ChIP-F	CCAAAGAATAGTCGTAGCCGCCG
CCNA2-ChIP-R	TCGAGCTGGGTGAGCGAGC
CDC20-ChIP-F	CGGTTGGATTTTGAAGGAGCC
CDC20-ChIP-R	CAGTTCCGACCGGCTTTAAC
CDC45-ChIP-F	CGGGCGGA ACTAAGCTACAA
CDC45-ChIP-R	CTGGGAACCCTCAGGGAAAG
IDH3A-ChIP-F	TGTCTTTCTCCACGGGATTG
IDH3A-ChIP-R	GACGTTTGTTCACACCTACTA
IDH3B-ChIP-F	GCACTTTGTCTCTTGCTTTG
IDH3B-ChIP-R	TCAGGTCCTCGTCTGATAAA
IDH3G-ChIP-F	GTCAGTGCTGCCAGAGA
IDH3G-ChIP-R	AAGAGCGACGCGTAAGT

**Table S7. Oligonucleotides used for luciferase reporter construction**

Oligo	Sequence (5'-3')
IDH3A promoter -HAF	GCTCGAGATCTGCGATCTAAGAGTCTCTGTTCCAGAAACAA CGTCA
IDH3A promoter -HAR	TTTACCAACAGTACCGGAATGGAGGCTCCCGTGACCTTCCC
IDH3B promoter -HAF	GCTCGAGATCTGCGATCT TCCTGTACCAGTTTGTCTTTAGG
IDH3B promoter -HAR	TTTACCAACAGTACCGGACAGTTGACTTTGCCCTGTTTAG
IDH3G promoter -HAF	GCTCGAGATCTGCGATCTCCTTGCCTTAGCCTTCTCCATAA C
IDH3G promoter -HAR	TTTACCAACAGTACCGGAGTGGCTCTTTCCCTGCTCAC
CCNA2 promoter -HAF	GCTCGAGATCTGCGATCTGCTGTAACCAGTGGAGCTATT
CCNA2 promoter -HAR	TTTACCAACAGTACCGGACACTCTTCTCTGCCTGCTAAG
CDC20 promoter -HAF	GCTCGAGATCTGCGATCTGATGGTCTCGATCTTCTGACTTC
CDC20 promoter -HAR	TTTACCAACAGTACCGGAGTGCAGGTCCTCTCGAAC
CDC45 promoter -HAF	GCTCGAGATCTGCGATCTTCAACTCTCCAGTCCCTACTT
CDC45 promoter -HAR	TTTACCAACAGTACCGGATCAAGACTCCCGCCAAATC

**Table S8. GSEA report for MYC targets genes**

<b>Name</b>	<b>Size</b>	<b>ES</b>	<b>NES</b>	<b>p-value</b>	<b>FDR, q-value</b>	<b>FWER, p</b>
HALLMARK_MYC_TARGETS_V1	195	0.197687	0.864773	0.774446	0.816426	1
HALLMARK_MYC_TARGETS_V2	58	0.288255	1.045651	0.395385	0.42958	1